

V 3903 Sagittarii: a massive main-sequence (O7V+O9V) detached eclipsing binary[★]

L.P.R. Vaz^{1,3}, N.C.S. Cunha¹, E.F. Vieira^{2,1}, and M.L.M. Myrrha¹

¹ Departamento de Física, ICEx, UFMG, Caixa Postal 702, 30.161-970 Belo Horizonte MG, Brazil

² European Space Agency-ESA, Villafranca del Castillo, Apdo. 50727, E-28080 Madrid, Spain

³ Department of Astronomy, University of Wisconsin, Madison, Wisconsin 53706, USA

Received 22 May 1997 / Accepted 11 July 1997

Abstract. We present for the first time an analysis based on *wby* light curves, $H\beta$ indices and on new spectroscopic data of the massive detached double-lined O-type eclipsing binary V 3903 Sgr. The *wby* light curves are analysed with the WINK (initial solutions) and the Wilson-Devinney (WD, final solution) programs. Both codes were used in their extended versions, with stellar atmospheres and taking into account the geometric distortions and photometric effects caused by proximity of the components.

The spectroscopic CCD observations were analysed with the harmonic “Wilsing-Russell” and the “Lehman-Filhes” methods. We conclude that V 3903 Sgr is one of the rare O-type detached systems where both components are still on the initial phases of the main sequence, with an age of either 1.6×10^6 yrs or 2.5×10^6 yrs (depending on the evolutionary model adopted) at a distance of ≈ 1500 pc, the same as for the Lagoon Nebula (Messier 8) complex, of which the system is probably a member. We determine the absolute dimensions: $M_A = 27.27 \pm 0.55$, $R_A = 8.088 \pm 0.086$, $M_B = 19.01 \pm 0.44$ and $R_B = 6.125 \pm 0.060$ (solar units). There is no evidence of mass transfer and the system is detached. The orbit is circular, and both components show synchronous rotation, despite their early evolutionary stage. The absolute dimensions determined should be representative for normal single stars. Amongst the massive systems ($M > 17M_\odot$) with precise absolute dimensions (errors $< 2\%$), V 3903 Sgr is that with the most massive primary, with the largest mass difference between the components, and it is the youngest one.

Key words: binaries: eclipsing – stars: individual: V 3903 Sgr; early type; fundamental parameters

1. Introduction

The eclipsing character of V 3903 Sgr was discovered by Cunha et al. (1990), the primary minimum having an amplitude of $0^m 18$, $0^s 02$ deeper than the secondary in the *y* passband. Cousins (1973) and Clariá (1976) both reported variations in the brightness of the system, classifying it as an irregular variable, but no light curve was published. Laurenti & Cerruti (1990) communicated UBVR observations with very large scatter.

The system is a known spectroscopic binary (Conti & Alschuler 1971, Niemela & Morrison 1988), and very possibly a member of the R association Simeis 188 (Herbst et al. 1982, Cunha 1990, Vaz et al. 1993). High-precision photometric (*wby*) and spectroscopic observations are used in the present work. No sign of orbital eccentricity or period variation was found in our analysis. Information concerning V 3903 Sgr and the comparison stars is given in Table 1. The system is close to the Lagoon Nebula ($\alpha_{1950} = 18^h 00^m$, $\delta_{1950} = -24^\circ 23'$) and to Sagittarius OB1 association (centered at $\alpha_{1950} = 18^h 05^m$, $\delta_{1950} = -21^\circ 28'$).

Responding to the lack of data on accurate masses and radii of O stars (Andersen 1993), we secured complete *wby* light curves of V 3903 Sgr (Vaz et al. 1997), additional $H\beta$ photometry, and spectroscopic observations, that are presented here together with their analysis. Our results show that V 3903 Sgr is a well detached system, suited for precise determinations of masses and radii of its components. As the initial quality and distribution of our data obtained at PDO-LNA-CNPq were not adequate for very high precision determinations, we obtained more *wby* observations at ESO, La Silla, with the SAT telescope. Both sets of photometric observations are analysed in this work (see Vaz et al. 1997 for a comparison between them).

2. Spectroscopic analysis

V 3903 Sgr was observed between 1989 and 1992 with the 1.6 m telescope and coude spectrograph at Pico dos Dias Observatory (PDO), National Laboratory for Astrophysics (LNA-CNPq) at Brasópolis-MG, Brazil. From 1989 to 1991 an EEV CCD

Send offprint requests to: L.P.R. Vaz at address 1 or at lpv@fisica.ufmg.br

[★] Based on data collected with the 60 cm and 1.6 m telescopes at the Pico dos Dias Observatory, National Laboratory of Astrophysics, LNA-CNPq, Brasópolis, MG, Brazil and with the Danish 50 cm telescope (SAT) at the European Southern Observatory (ESO), La Silla, Chile

Table 1. Catalogue data and standard $uvby\beta$ indices for V 3903 Sgr and the comparison stars. The indices for V 3903 Sgr are for phases 0^h7^m5 (uvby) and 0^h22 (β).

	V 3903 Sgr	C ₁	C ₂	C ₃	C ₄
HR	-	-	-	6 724	6 835
HD	165 921	165 999	164 681	164 584	167 666
SAO	186 366	186 375	186 160	186 163	186 594
DM	-24° 13 962	-23° 13 991	-26° 12 724	-24° 13 793	-28° 13 407
Sp	O7V+O9V	A5III	A4V	F5II	A4III
α_{1950}	18 ^h 06 ^m 14 ^s	18 ^h 06 ^m 33 ^s	18 ^h 00 ^m 17 ^s	17 ^h 59 ^m 47 ^s	18 ^h 14 ^m 13 ^s
δ_{1950}	-23°59'52''	-23°34'40''	-26°19'18''	-24°17'01''	-28°40'17''
l	6°9	7°3	4°3	6°0	3°7
b	-2°1	-2°0	-2°1	-1°0	-5°9
V	7.271 ±6	7.683 ±8	7.340 ±10	5.408 ±9	6.198 ±6
$b - y$	0.186 ±2	0.170 ±4	0.071 ±4	0.336 ±6	0.114 ±5
m_1	0.004 ±5	0.142 ±2	0.122 ±7	0.140 ±4	0.162 ±9
c_1	-0.102 ±9	1.096 ±9	1.038 ±9	1.030 ±11	1.145 ±13
β	2.584 ±2	2.869 ±4	2.879 ±6	2.709 ±6	2.852 ±3

(386×576 22 μm square pixels) P8603S chip was used with a model #1 (serial no. 48) camera and acquisition program (AT1, version 3.1) from Wright Instruments Ltd. The mean dispersion was 18.1 Å/mm (0.397 Å/pix, corresponding to ~230 Å covered in each frame), with a projected slit width of 1.40 pixel. Average exposure times were from approximately 10 min at 6600 Å to 20 min at 4400 Å. The grating (Milton Roy Co.) used in this observing period has 600 lines/mm blazed for 8000 Å (13°53'). The observations in 1992 were done with a 1800 lines/mm holographic grating (Jobin Yvon) blazed from 3000 Å to 7500 Å and with an EEV CCD 05-20-0-202 (770×1152 22.5 μm square pixels, grade 0) chip with UV coating at a mean dispersion of 5.84 Å/mm (0.131 Å/pix, ~150 Å covered in a frame), with a projected slit of 1.37 pixel. All spectra of 1992 were exposed for 20 min. We reduced all spectra by using a C computer program implemented by Vieira (1991, 1993) using the optimum extraction algorithm by Horne (1986).

After analysis of the results from several individual lines, as described by Andersen (1975), the He lines listed in Table 2 were found to give consistent velocities. The diffuse He I lines have been found to give systematic errors of ~ 10% in mass for other OBA-type binaries (e.g. Andersen et al. 1980), but the lack of lines in the short-wavelength region and the orbital phase distribution of the spectra forced us to use them. However, as we are using a significant number of sharp lines, the effect mentioned above should be small and will be neglected. As a matter of fact, starting from the adopted solution (Table 4)

Table 2. He lines measured in V 3903 Sgr

Wavelength (Å)	lines	note
4387.928	He I	D
4471.477	He I	D
4541.590	He II	S
4685.682	He II	S
5015.675	He I	S
5047.736	He I	S
5875.752	He I	S
6678.149	He I	S

D = diffuse; S = sharp

and using only the present observations obtained with the sharp lines, the final elements remained practically unchanged, with only the errors becoming larger (by approximately 20%) due to the smaller number of points.

2.1. Radial-velocity curves and the mass ratio

After reduction and calibration of the spectra, radial-velocity measurements were made by (least-squares) fitting double lorentzian and/or gaussian curves as described by Myrrha (1991, procedure used in LZ Cen, Vaz et al. 1995, and V906 Sco, Alencar et al. 1997, also) in order to find the observed center of the

lines of Table 2. Our (PDO) spectra do not cover more than 230Å in each frame and it is difficult to use cross-correlation functions (e.g. Hill & Khallesseh 1991), as would be preferable. However, we did use cross-correlation techniques to obtain the last point of Table 3 (CTIO echelle spectra), which is in very good agreement with the rest of our data, showing that we did take correct account of the effects of blending. The fits were done on the normalized spectra, after determination of the continuum. Fig. 1 shows part of the normalized spectrum of V 3903 Sgr for the phases $\phi=0.21$ and $\phi=0.62$.

Many interstellar lines are seen in the spectra, as shown in Fig. 1; the single pair of Na I interstellar lines appear at a velocity of -1.8 ± 0.1 km/s. V 3903 Sgr is possibly the illuminating star of the bright nebula IC 4685 (Hirshfeld & Sinnott 1982, 1985), and it is not unexpected that we detected so many interstellar lines. On the other hand, it is surprising not to have found more than one resolved component of the Na I pair, due to the position of the system in the galactic plane (Table 1) and its distance to the Sun (~ 1500 pc, see Table 10). Probably this is due to the fact that in the direction of the Galactic Centre, all the motion is transverse and not radial, and so any interstellar velocity will be small (Stickland 1996).

The measured radial velocities are shown in Fig. 2 and in Table 3, where the last point is one measurement obtained with the 1.5 m telescope at CTIO equipped with the bench-mounted echelle spectrograph (see Sect. 2.2). The columns 4 and 7 of Table 3 (labelled “w”) indicate if the observations were used (1) or not (0) in the solutions. Excepting the last point, which was determined using a different instrument and procedures, all the observations of Table 3 were obtained through a homogeneous process and those which received zero weight were blended and/or underexposed. The proximity effects on the measurements are modeled as described by Wilson and Sofia (1976) in the WD code used to analyse the light curves (Sect. 3.3). Velocity corrections for the observed phases have been computed with the final model parameters adopted for V 3903 Sgr (Sect. 3.3.2) and were included in the (O-C) columns of Table 3 (columns 5 and 8, but are **not** included in the observed data, columns 3 and 6).

The adopted spectroscopic solution is given in the last column of Table 4 and is shown as a solid line in Fig. 2. The solutions of the spectroscopic elements were performed both with a C program (written by NCS) based on the harmonic “Wilsing-Russell” method (Wolfe Jr. et al. 1967) and using the FORTRAN program SBOP (Etzell 1985) which allows solutions with the methods of Lehmann-Filhes (1894) and Sterne (1941), also. The solutions were performed with four different procedures: the Wilsing-Russell and Sterne methods applied to each component separately, and solving for both components simultaneously with Lehmann-Filhes method; the fourth is the WD method, used in Sect. 3.3.2 to solve simultaneously the *woby* colours **and** the radial-velocity curve of each component. Our results with these different methods agree very well with each other and we adopt the simultaneous solution for both components with the Lehmann-Filhes method, as described below.

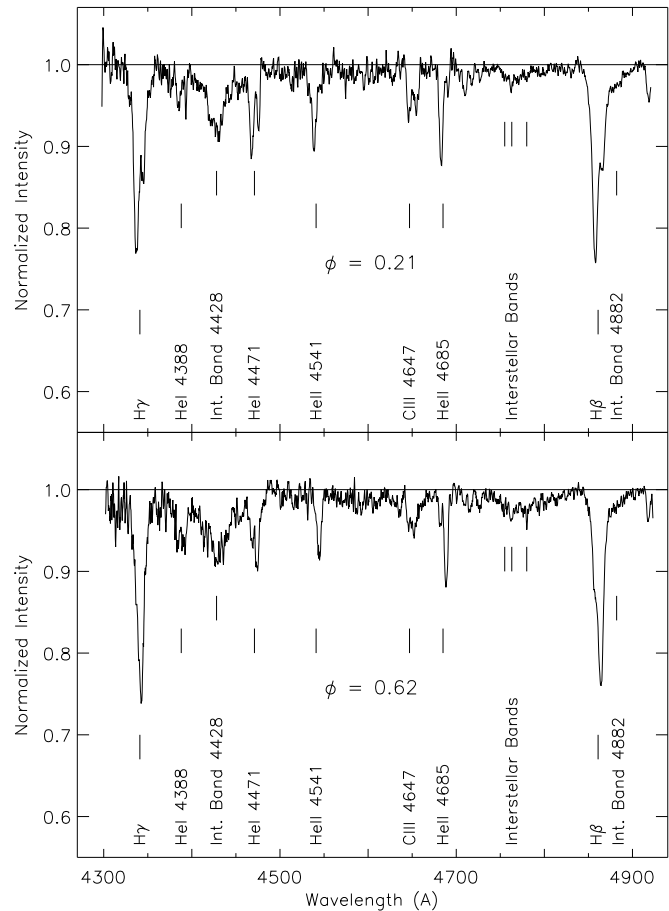


Fig. 1. Rectified spectra of V 3903 Sgr at phases $\phi = 0.21$ and $\phi = 0.62$ with identified lines. Each CCD frame was $\sim 200\text{\AA}$ wide, and each figure shows a combination of three individual CCD frames. Note the large number of interstellar features. The spectra were smoothed with a boxcar of 5 pixels.

In Table 4 we present solutions (Lehmann-Filhes applied to both components simultaneously) performed only with the non-zero weight observations of Table 3 (solutions 1 and 2). We applied this method to Niemela & Morrison observations alone (also shown in Fig. 2) and reproduced their published solution (1988), which agrees well with solution 2 of Table 4. Therefore we decided to combine our data (Table 3) with those by Niemela & Morrison (1988), generating the solutions 3 and final. In solutions 1 and 3 we left e , the orbital eccentricity and ω , the angle of periastron passage, free to be adjusted. Table 4 gives T_0 for solutions 1 and 3 (free e , ω) as the time of periastron passage, while in the circular orbit solutions (2 and final) T_0 is the time of conjunction, given by the adopted ephemeris (Sect. 3.1). Even though the formal errors of both e and ω are small enough to make the value significant, we notice that the values of ω in solutions 1 and 3 are very different, indicating that the orbital eccentricity may be an artifact of the data. Therefore we assumed a circular orbit, what is supported by the photometric observations, as described in Sect. 3, which give no indication of an eccentric orbit. Niemela & Morrison (1988) also assume a

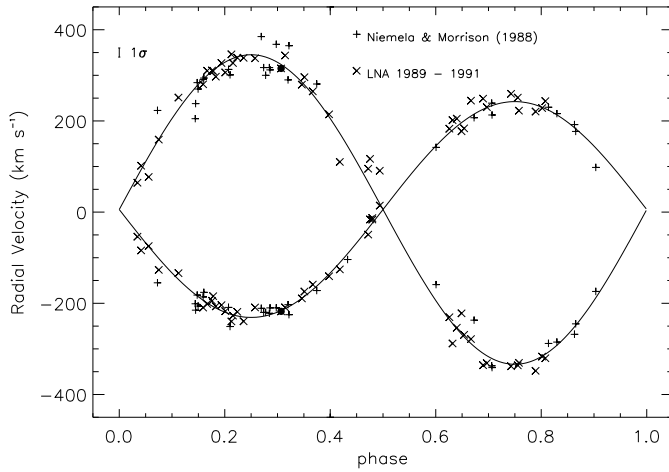


Fig. 2. Observed and theoretical radial-velocity curves of V 3903 Sgr. The bar at the upper left part of the figure is the mean error ($\sigma = 20 \text{ km s}^{-1}$) of 1 observation in our measurements. \times symbols correspond to PDO observations, \bullet to the measurements obtained at CTIO and $+$ to observations by Niemela & Morrison (1988) used in the solution (only observations with non-zero weights in Table 3 are shown).

circular orbit in their solution for the system. Although the σ (1 obs.) for the adopted solution is the largest of Table 4, it is compatible with the intrinsic error of our observations (20 km/s).

The adopted solution of Table 4 yields the mass ratio q ($= M_B/M_A$) = 0.697 ± 0.010 , essentially the same result given by the WD model in the simultaneous solutions of Sect. 3.3.2. This value agrees with and improves Niemela & Morrison's (1988) determination, $q = 0.709 \pm 0.025$.

2.2. Rotation rates and luminosity ratios

We are in debt to Dr. R.D. Mathieu, who very kindly took some spectra of V 3903 Sgr and rotational standard stars with the 1.5 m telescope of Cerro Tololo Interamerican Observatory (CTIO) and the bench-mounted echelle spectrograph described in Casey et al. (1992). The observations were made in June 26, 1994 and were reduced by Dr. N.B. Suntzeff using IRAF, which is gratefully acknowledged. The widths (FWHM) of the same lines in V 3903 Sgr were interpolated between those in the rotational standard stars (Slettebak et al. 1975) HR 6175 (O9.5V, $v \sin i=400 \text{ km/s}$, see below), HR 6165 (B0V, $v \sin i < 10 \text{ km/s}$), HR 5953 (B0.3IV, $v \sin i=150 \text{ km/s}$) and HR 6462 (B1Ib, $v \sin i=230 \text{ km/s}$). The resulting mean rotational velocities for the two components of V 3903 Sgr are $v_A \sin i=230 \pm 23 \text{ km/s}$ and $v_B \sin i=170 \pm 17 \text{ km/s}$, confirming measurements based on the same rotational standards made with the PDO's equipment. As the dispersion of CTIO echelle spectra is significantly higher than those for the traditional Coudé ones taken at PDO, we adopt the result above for the rotational projected velocities.

It should be mentioned that the CTIO echelle spectra showed asymmetries in most of the detected lines of both HR 5953

Table 3. Radial velocity observations of V 3903 Sgr.

HJD - 2 440 000	phase	star A w (km/s)	O-C (km/s)	star B w (km/s)	O-C (km/s)
7753.5503	0.4720	-49.3 1	-13.5	95.2 0	19.0
7753.5639	0.4798	-13.0 1	11.3	16.4 0	-41.0
7754.5314	0.0345	-53.8 1	0.6	64.5 1	-13.8
7754.5436	0.0415	-84.0 0	-19.2	101.7 1	9.0
7754.5686	0.0558	-74.4 1	9.3	77.2 0	-44.6
7754.6020	0.0749	-126.7 0	-20.5	159.0 1	0.0
7756.4928	0.1590	-209.4 1	-15.7	280.3 1	-8.9
7756.5224	0.1760	-194.5 1	11.0	310.6 1	3.8
7756.5348	0.1831	-206.6 1	3.2	297.1 1	-16.1
7756.5662	0.2011	-217.3 1	1.3	306.3 1	-20.3
8021.6726	0.1938	-204.0 1	11.4	327.1 1	5.4
8021.7106	0.2156	-222.7 1	1.0	327.0 1	-7.5
8021.7248	0.2238	-218.7 1	7.0	338.7 1	0.9
8021.7457	0.2357	-239.5 1	-11.8	338.3 1	-2.7
8079.4971	0.3462	-189.4 1	-1.7	279.6 1	-4.0
8079.5057	0.3511	-174.2 1	9.4	295.9 1	18.3
8079.5332	0.3669	-158.8 1	10.3	264.9 1	8.2
8079.6226	0.4182	-125.6 1	-15.0	110.1 0	-65.2
8079.7547	0.4939	14.4 1	17.8	90.8 0	70.0
8081.7291	0.6259	183.0 1	9.8	-230.5 1	4.2
8081.7396	0.6319	201.6 1	22.4	-288.1 0	-44.6
8081.7693	0.6489	177.3 1	-17.6	-222.1 0	44.1
8081.7778	0.6538	183.7 1	-15.3	-269.1 1	3.0
8081.8005	0.6668	244.5 0	35.4	-278.4 1	8.3
8440.6372	0.3978	-140.7 1	-4.9	214.5 1	5.8
8442.5171	0.4755	-16.1 1	14.5	116.8 0	49.1
8498.6182	0.6399	205.0 1	18.2	-253.5 1	1.0
8499.4424	0.1123	-133.9 1	15.8	251.3 1	26.6
8499.5369	0.1666	-201.5 1	-2.2	310.0 1	12.6
8499.6174	0.2127	-239.8 1	-17.0	346.1 1	12.6
8500.4496	0.6898	248.9 1	25.5	-335.8 1	-28.2
8500.4619	0.6969	230.2 1	3.2	-331.2 1	-18.5
8500.5681	0.7577	222.5 1	-17.3	-330.6 1	-0.0
8500.6447	0.8017	228.2 1	-0.8	-316.9 1	-3.4
8813.5138	0.1781	-184.4 1	22.5	309.4 1	0.6
8813.6521	0.2574	-209.1 1	19.0	337.5 1	-4.5
8813.7517	0.3145	-209.0 1	0.7	343.6 1	28.0
8814.4987	0.7428	259.5 1	19.9	-338.0 1	-7.4
8814.5208	0.7555	251.2 1	11.3	-336.1 1	-5.4
8814.5798	0.7893	220.6 1	-13.1	-348.1 1	-27.3
8814.6121	0.8078	243.4 1	17.2	-320.4 1	-11.2
9530.6062	0.3068	-217.7 1	-3.9	315.1 1	-6.5

(δ Sco) and HR 6175 (ζ Oph), especially conspicuous in $H\alpha$ and $H\beta$ lines. ζ Oph is known to have line-profile variability caused by non-radial pulsations (Walker et al. 1979, Janot-Pacheco et al. 1991). Its rotation rate was determined by Reid et al. (1993) to be $v \sin i=400 \pm 20 \text{ km/s}$. ζ Oph is a prototype giving its name to the subclass of stars with similar line-profile variability behaviour (Balona 1990). For δ Sco the asymmetries observed suggest the occurrence of double lines. If this duplicity is real, it indicates velocity differences as large as $110 \pm 20 \text{ km/s}$. Naturally, the status of standard for rotation velocities of this star should be revised if this duplicity is confirmed.

Table 4. Spectroscopic solutions for V 3903 Sgr. Adopted final orbital elements are in the last column.

Element	sol. 1	sol. 2	sol. 3	adopted
(N)	(82 observations)		(150 observations)	
P	$1^d7442360$ ± 76	$1^d744204$ (fixed)	$1^d7442068$ ± 23	$1^d744204$ (fixed)
T_0 (-2 440 000)	7394^d52 ± 15	7754^d4713 (fixed)	7100^d841 ± 88	7754^d4713 (fixed)
e	0.0173 ± 85	0.000 (fixed)	0.0225 ± 71	0.000 (fixed)
ω_{primary} ($^\circ$)	317 ± 31	90 (fixed)	184 ± 18	90 (fixed)
V_0 (km s^{-1})	4.5 ± 1.8	4.9 ± 1.8	5.5 ± 1.4	5.7 ± 1.6
K_A (km s^{-1})	237.0 ± 3.1	237.6 ± 3.1	236.7 ± 2.5	236.6 ± 2.7
K_B (km s^{-1})	341.8 ± 3.2	342.6 ± 3.2	337.7 ± 2.7	339.4 ± 2.8
$a_A \sin i$ (R_\odot)	8.17 ± 11	8.19 ± 11	8.156 ± 87	8.154 ± 93
$a_B \sin i$ (R_\odot)	11.78 ± 11	11.81 ± 11	11.633 ± 92	11.623 ± 98
$M_A \sin^3 i$ (M_\odot)	20.69 ± 38	20.84 ± 38	20.12 ± 30	20.36 ± 32
$M_B \sin^3 i$ (M_\odot)	14.35 ± 29	14.43 ± 29	14.11 ± 24	14.19 ± 25
M_B/M_A	0.693 ± 11	0.693 ± 11	0.701 ± 9	0.697 ± 10
$\sigma(1 \text{ obs.})$	15.9	16.1	17.0	18.3

The ratio of the equivalent widths of the relatively unblended He I lines of Table 2 for both components was measured yielding $EW_B/EW_A = 0.441 \pm 0.074$. The temperatures of both stars in V 3903 Sgr are significantly different and, therefore, it is not straightforward to associate the ratio of equivalent widths directly with the luminosity ratio. However, it is expected that the intensity of the He I lines decreases with increasing temperature and that the ratio of equivalent widths above is in fact an upper limit for L_B/L_A . Using He II at 4686 Å and the CTIO spectra, we obtain 0.242 ± 0.014 , which should be a lower limit for the actual value of L_B/L_A .

3. Photometric analysis

3.1. Observations

The photometric observations were obtained at two different sites: (1) from 1989 to 1991 at PDO (LNA-CNPq, Brasópolis, Brazil), with the ZEISS 60 cm telescope and a single-channel photometer equipped with a photon-counting system and using a diaphragm of 39'' diameter (Cunha et al. 1990); and (2) from 1990 to 1994 at ESO (La Silla, Chile), with the

Strömgren Automatic Telescope (SAT) equipped with the six-channel spectrograph-photometer and photon-counting system described by Nielsen et al. (1987). In the measurements taken from 1990 to 1993 with SAT, a circular diaphragm of 13'' diameter was used, but in 1994 observations the 17'' diameter diaphragm was used. All observations are published in a separate paper (Vaz et al. 1997) where the reduction procedure is described.

HD 165 999, HD 164 681, HD 164 584 and HD 167 666, all relatively close to V 3903 Sgr (Table 1), were used as comparison stars in all observing runs and observed alternately between the measurements of the variable. All four stars were found to be constant within the observational accuracy throughout the observing periods in both sites.

The PDO light curves, u (478 points), v (532), b (544) and y (537), are shown in Vaz et al. (1997). Typical rms errors of one magnitude difference between the four comparison stars were: 0^m009 , for $\sigma(\Delta u)$, 0^m006 (Δv), 0^m005 (Δb and Δy). The SAT y light curve, the $(b - y)$ and $(u - b)$ colour indices curves (687 observations in each colour) are shown in Fig. 3 and the typical rms errors of one magnitude difference between the comparison stars were: 0^m006 (Δu), and 0^m003 (Δv , Δb , Δy). Note that in Fig. 3 all observations made with SAT are shown, and the effect of changing the size of the diaphragm is surprisingly small, as the region is very close to bright nebulae (Lagoon Nebula and IC 4685) which could contaminate the observations with spurious light. This contamination is perhaps noticed in the observations made in 1990, mainly in the shoulders of the primary eclipse (JD-2 440 000=)8019, covering phases 0:14 to 0:20, and 8029, covering phases 0:82 to 0:94). However, night 8016 (0:45 to 0:48) and the primary eclipse part of 8029 do match the 1994 observations very well (in Vaz et al. 1997).

3.2. Ephemeris and period analysis

From the present observations, we determined the times of minima given in Table 5, by applying the method of Kwee & van Woerden (KvW, 1956) to all four colours and controlling the results with second and third degrees polynomials. The mean of the four measures was adopted, with an uncertainty derived from their internal rms dispersion.

With the Lafler and Kinman (1965) period-search method applied to the PDO observations we determine the period $P=1^d744203 \pm 0^d000004$. By applying the method to (all) SAT observations we find $P=1^d744205 \pm 0^d000003$. Applying the method to all (PDO and SAT) observations combined, the result is $P=1^d744204 \pm 0^d000003$. By using the least-squares method and linear ephemeris to minimize the O-C of the prediction of times of minima, given in Table 5, we find the periods: $P=1^d744199 \pm 0^d000008$ (primary minima) and $P=1^d74422 \pm 0^d00010$ (secondary minima), which are in good agreement with each other and with our period search determinations. Introducing a quadratic term in the procedure does not change the numbers significantly and the second order coefficients turn out to be very small (5×10^{-9} for the primary minima

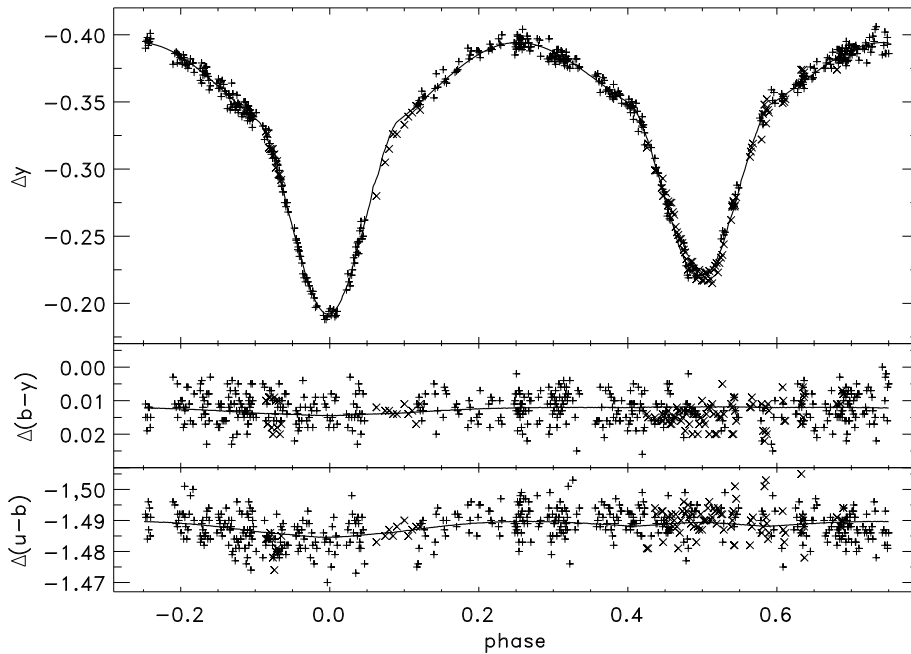


Fig. 3. y , $b - y$ and $u - b$ magnitude differences V 3903 Sgr–HD 165999 obtained at ESO and the theoretical light curves (Table 10, \times : observations made from 1990 to 1993 with a diaphragm of $13''$, $+$: observations made in 1994 with a diaphragm of $17''$).

Table 5. Times of minima for V 3903 Sgr.

HJD–2 440 000	type	O-C	E
7691.6813 ± 0.0019	pri	$+0^d.0013$	-36.0
7754.4713 ± 0.0005	pri	$+0^d.0000$	0.0
8107.6655 ± 0.0002	sec	$-0^d.0071$	202.5
8108.5454 ± 0.0005	pri	$+0^d.0007$	203.0
8115.5246 ± 0.0005	pri	$+0^d.0031$	207.0
8372.7977 ± 0.0017	sec	$+0^d.0061$	354.5
8400.6960 ± 0.0002	sec	$-0^d.0029$	370.5
8401.5719 ± 0.0002	pri	$+0^d.0009$	371.0
8407.6761 ± 0.0002	sec	$+0^d.0004$	374.5
8420.7580 ± 0.0001	pri	$+0^d.0008$	382.0
8421.6308 ± 0.0003	sec	$+0^d.0015$	382.5
9538.7895 ± 0.0002	pri	$-0^d.0025$	1023.0
9539.6638 ± 0.0007	sec	$-0^d.0003$	1023.5
9545.7661 ± 0.0009	pri	$-0^d.0027$	1027.0

and 5×10^{-8} for the secondary ones) and barely larger than their formal errors. Therefore we adopt the new ephemeris:

$$\text{Min I at: HJD } 2\,447\,754.4713 + 1^d.744204 E \\ \pm 5 \quad \pm 6$$

The most distant reference we have of an orbital phase for the system is the time of maximum radial velocity (at phase $0^d.25$, cycle -1469.25, as referred to our new determined ephemeris). If we add this to the analysis above, we again find the period $P = 1^d.744199 \pm 0^d.000008$. However, the rms of the O-C increases by a factor of 3. The two periods are essentially equivalent, considering their errors, and we will use the one given in the ephemeris above.

3.3. Photometric analysis

The light curves were solved initially with the WINK (Wood 1971, Vaz 1986) model and the final solutions were found with the more realistic WD (Wilson 1979, 1993) model. Both models were improved with the modifications described by Vaz et al. (1995). The system turned out to be detached, with both components still well inside their Roche Lobes. Models using simpler approximations for the geometric figure of the components, like EBOP (Popper & Etzell 1981), are not adequate for the analysis of this system, which presents moderate proximity effects (Fig. 3).

Only PDO light curves were used to find initial solutions, because they were completed before the ESO ones.

3.3.1. Starting values and initial solutions

We studied the possible values for the orbital inclination, i , so that the system would be detached, but close to the contact configuration (a starting hypothesis, Cunha 1990), concluding that i should be close to 65° . For normal O7V and O9V stars (Niemela & Morrison 1988) Popper's (1980) work indicates that the ratio of radii should be close to 0.8, which we used as our initial value for $k (= r_B/r_A)$. The photometric standard indices (Table 1) give a mean system temperature close to 35 000 K (Lester et al. 1986). The unreddened combined $[m_1]$ index is consistent with an O8V spectral type for the system, while $[c_1]$ disagrees with any calibration. The system is far too hot for the use of the calibrations by Napiwotzki et al. (1993) and Schönberner & Harmanec (1995). We then took the temperature starting values to be 38 000 K and 33 000 K as adequate for the spectral types O7V and O9V, respectively, according to the works of Conti (1973) and Lamers (1981).

The intrinsic $(B - V)$ index for these temperatures is -0.31 (Morton 1969, Popper 1980). There is a well defined empirical relation between $(B - V)$ and $(b - y)$ for O stars with small interstellar reddening (Crawford 1975 using his own observations and measurements by Hiltner & Johnson 1956): $(B - V) = -0.069 + 1.347(b - y)$. Using this relation and the observed $(b - y)$ from Table 1 we find $(B - V)_{\text{obs}} = 0.18 \pm 0.07$, yielding $E(B - V) = 0.49 \pm 0.07$. By using a normal total to selective extinction, $A_V = 3.17 E(B - V)$ (e.g. Seaton 1979), we find $A_V = 1^m55 \pm 0.23$ (the error is dominated by the uncertainty in $(B - V)_0$ and by the dispersion in the $(B - V)$ versus $(b - y)$ relation above).

We fixed $T_{\text{eff},A}$ at 38 000 K and left $T_{\text{eff},B}$ to be adjusted by the least-squares method. The reflection albedos were fixed at 1.0 and the gravity darkening exponents were chosen to follow von Zeipel's (1924) work, as appropriate for atmospheres in radiative and hydrostatic equilibrium.

The limb-darkening coefficients were initially taken from Wade and Ruciński (1985) and then from the tables of Van Hamme (1993), both for Kurucz (1979) stellar model atmospheres and calculated by bi-linear interpolation at the current values of T_{eff} and $\log g$. As Van Hamme's (1993) tables do not cover the region with $\log g < 4.5$ for temperatures above 35 000 K, we extrapolated the values of limb-darkening in this region, always taking into account the general pattern of variation of the limb-darkening coefficient for the listed values of $\log g$ and T_{eff} . For these hot temperatures, this procedure should be sufficiently precise (Van Hamme 1995).

Even though V 3903 Sgr is in a rich field close to bright nebulae, no other star could be detected inside the diaphragm with an image intensifier and no third light was assumed in the initial solutions. At first we assumed synchronous rotation for both components. Their rotation velocities (Sect. 3.2) were then used to calculate the rotation rates relative to the orbital movement, on which the sizes and deformations of both components depend.

Starting with these initial values and the y light curve which presents the least dispersion, we applied the WINK model to a normal curve (39 points strategically distributed along the orbital phases), obtained from the observations with a spline interpolation curve. As soon as a physically plausible solution was achieved for the y colour, we added the bvu normal light curves to the analysis.

Both components were found to be well inside their Roche lobes, and the preliminary solutions given in Table 6 were found. One can see that the solutions agree well in all four colours. The limb-darkening coefficients for the u colour, however, was increased by 0.1 for both components, in order to get a better agreement of the orbital inclination for this colour with those found for the other colours. This tendency has already been noted in other works on hot (B) stars, such as Giménez et al. (1986), Vaz et al. (1995), and references cited in these works.

Table 6. Initial solution for V 3903 Sgr, obtained with the WINK model and PDO observations.

parameter	y	b	v	u
i	63°012	63°041	62°984	62°782
r_A	0.362	0.363	0.363	0.361
r_B	0.298	0.300	0.298	0.298
T_A (K, fixed)	38000	38000	38000	38000
T_B (K)	32158	32095	32374	32564
$\log g_A$ (cgs)	4.104	4.098	4.104	4.105
$\log g_B$ (cgs)	4.085	4.082	4.083	4.088
x_A	0.196	0.212	0.239	0.344
x_B	0.219	0.240	0.266	0.371
L_B/L_A	0.521	0.529	0.523	0.502

3.3.2. Final solutions with the WD model

The initial solutions indicate that V 3903 Sgr is moderately distorted, and that WINK probably generates a good representation for the components. However, due to its more accurate geometric approximation for the figure of the components, we decided to apply the WD model, first to the normal curves and then to all SAT observations, to find the final solutions. PDO observations were also analysed with the WD model, but not used in the final solution, as explained below. The code of the WD model was modified as described by Vaz et al. (1995), where they discuss in some detail the usefulness of the improvements.

Starting from the WINK solutions (Table 6) and using a set of UNIX scripts and small FORTRAN programs (Vaz et al. 1995), developed to make sure that *all* of the model parameters were integrally consistent both with the observed quantities and with themselves internally, the detached configuration was confirmed by the WD model, applied to SAT observations. No contact or semi-detached configuration could reproduce the observed light curves so well as the detached configuration. The solutions were performed on different sets, shown in Table 7: (1) applying WD simultaneously to all 4 colours (wby), (2) to the vby , (3) and (4) only to the u colour (solutions 1 to 4 used only SAT observations). Solutions (5, wby) and (6, vby) were done with PDO observations, and correspond to solutions (1) and (2), done with SAT observations, respectively. Solution (7) solves simultaneously all SAT wby light curves and the 2 radial velocity curves. The model input parameters $\mathcal{L}_{A,B}$ are 4π steradian luminosities (\mathcal{L}_B is automatically calculated from the input temperatures and radii), while L_3 is in units of the apparent light from the eclipsing stars integrated in the observer's direction.

The WD model was used with the atmosphere tables of Kurucz (1979), clearly a better approximation than the normal possibilities offered by the WD model: Carbon-Gingerich model atmospheres and the blackbody radiation approximation (see Vaz et al. 1995). Even though WINK uses the same set of atmosphere model tables, the better geometric approximation of the WD model gives an effective temperature of the secondary systematically higher (by more than 2 000 K, $\sim 6\%$) and an orbital inclination $\sim 2^\circ$ higher than those found in the initial solutions.

Table 7. Final solution for V 3903 Sgr, obtained with the WD model applied to all SAT (solutions 1, 2, 3, 4 and 7) and to PDO observations (solutions 5 and 6). Parameters marked (*) were kept consistent during iterations. The errors quoted are the least-squares formal errors.

param.	(1)	(2)	(3)	(4)	(5)	(6)	(7)
i	64°:924 ±33	64°:930 ±38	65°:32 ±11	65°:219 ±99	65°:534 ±38	64°:978 ±40	65°:200 ±65
Ω_A	3.5190 ±41	3.5177 ±46	3.468 ±82	3.5121 ±85	3.4490 ±43	3.6050 ±81	3.4889 ±68
Ω_B	3.6134 ±57	3.6157 ±69	3.729 ±19	3.685 ±18	3.7423 ±65	3.5322 ±87	3.696 ±12
T_A (K)	38000	38000	38000	38000	38000	38000	38000
T_B (K)	34185 ±25	34214 ±28	34027 ±52	34016 ±55	33682 ±33	33990 ±32	34117 ±35
a (R_\odot)	21.91 (fixed)	21.91 (fixed)	21.85 (fixed)	21.86 (fixed)	21.81 (fixed)	21.91 (fixed)	21.851 ±35
V_γ (km/s)	0.0 (fixed)	0.0 (fixed)	0.0 (fixed)	0.0 (fixed)	0.0 (fixed)	0.0 (fixed)	5.14 ±34
q	0.697 (fixed)	0.697 (fixed)	0.697 (fixed)	0.697 (fixed)	0.697 (fixed)	0.697 (fixed)	0.6993 ±15
$\mathcal{L}_{A,u}$	6.554 ±19	–	7.404 ±53	7.231 ±53	6.964 ±20	–	7.246 ±38
$\mathcal{L}_{A,v}$	6.275 ±19	6.274 ±22	–	–	6.690 ±19	5.988 ±33	6.944 ±36
$\mathcal{L}_{A,b}$	6.506 ±19	6.507 ±23	–	–	6.935 ±19	6.211 ±34	7.202 ±38
$\mathcal{L}_{A,y}$	6.599 ±20	6.602 ±23	–	–	7.030 ±20	6.295 ±35	7.313 ±38
$\mathcal{L}_{B,u}$	3.398	–	3.298	3.398	3.008	–	3.412
$\mathcal{L}_{B,v}$	3.364	3.358	–	–	3.013	3.600	3.387
$\mathcal{L}_{B,b}$	3.486	3.482	–	–	3.118	3.730	3.511
$\mathcal{L}_{B,y}$	3.563	3.559	–	–	3.190	3.816	3.591
$\log g_A^*$ (cgs)	4.070 ±14	4.070 ±14	4.051 ±14	4.067 ±14	4.053 ±14	4.097 ±14	4.058 ±14
$\log g_B^*$ (cgs)	4.116 ±13	4.116 ±13	4.157 ±13	4.141 ±13	4.161 ±13	4.085 ±12	4.143 ±13
$\frac{\omega_A}{\omega_{orb}}^*$	1.023 ±99	1.022 ±99	0.9995 ±99	1.019 ±99	1.008 ±100	1.061 ±99	1.005 ±98
$\frac{\omega_B}{\omega_{orb}}^*$	0.964 ±96	0.965 ±97	1.022 ±99	1.000 ±100	1.030 ±100	0.926 ±93	1.002 ±99
$r_{A,pole}$	0.3495	0.3497	0.3558	0.3495	0.3581	0.3396	0.3534
$r_{A,point}$	0.4000	0.4003	0.4125	0.4000	0.4064	0.3848	0.4079
$r_{A,side}$	0.3634	0.3636	0.3707	0.3634	0.3683	0.3536	0.3680
$r_{A,back}$	0.3809	0.3811	0.3898	0.3809	0.3862	0.3692	0.3865
$r_{B,pole}$	0.2790	0.2787	0.2669	0.2790	0.2656	0.2881	0.2710
$r_{B,point}$	0.3114	0.3109	0.2923	0.3114	0.2900	0.3245	0.2985
$r_{B,side}$	0.2868	0.2865	0.2734	0.2868	0.2717	0.2956	0.2779
$r_{B,back}$	0.3011	0.3007	0.2805	0.3011	0.2830	0.3118	0.2904
$\left(\frac{L_B}{L_A}\right)_{Bol}$	0.48 ±16	0.48 ±16	0.41 ±16	0.44 ±16	0.39 ±16	0.54 ±16	0.44 ±16
σ (mag)	0.0046	0.0043	0.0055	0.0055	0.0063	0.0051	0.0046

As happened with WINK (Sect. 3.3.1) the solution for the u colour (3) does not agree with the solution for the vby colours (2), with the main differences in the sizes of the stars, but also in the orbital inclination. These differences can be diminished by increasing the limb-darkening coefficient for the u colour, interpolated from Van Hamme’s (1993) tables, by 0.2 (Giménez et al. 1986, Vaz et al. 1995), as shown in solution (4). However, unlike the solution for LZ Cen (B1III, Vaz et al. 1995) and EM Car (O8V, Andersen & Clausen 1989), the discrepancy could not be completely removed with this procedure. Separate solutions were done for the individual vby (SAT) colours, which fully agree with solution (2).

We are using the two sets of observations we have in their own instrumental system so it is natural to expect some differences between solutions produced with SAT or PDO data, due to differences in the equipment, photomultipliers, filters, diaphragms and sites, even though the comparison stars were the same in both data sets. One consequence of these differences is that the light curve u from PDO was the only one which required the use of “third light”, of around 1.4% of the eclipsing components’ contribution at quadrature (according to WINK definition, implemented in WD as an option), in order to better reproduce the geometric elements for solutions of the vby colours. When this parameter, L_3 , was adjusted by the least-squares method for the vby light curves, it remained zero or became slightly negative, which is not physically reasonable. The diaphragm used in PDO observations was larger than both those used in SAT runs (Sect. 3.1, Vaz et al. 1997). Therefore, if there was any necessity of considering extra light in the solutions, the PDO solutions should use larger values than SAT ones, due to sky background contamination. However, it seems that the third light for u is an artifact created by the combination of instruments and site at PDO. By analysing the u filter transmission (both sites) it becomes clear that PDO u filter is approximately 15% broader than that used in SAT photometer. As V 3903 Sgr is of a much earlier spectral type than the comparison stars used (especially C₁, Table 1), this difference in the bandwidth alone could be the reason for this “artificial” third light in the u light curve.

Only solutions with the PDO u colour showed differences with respect to solutions with SAT data, as can be seen in Table 7, solutions (5) and (6) corresponding to the simultaneous solutions (1, $uvby$) and (2, vby), respectively. The vby light curve solutions are essentially the same for both data sets, considering the formal errors of the parameters. The inclusion of the u colour in solution (5) really produced another configuration (i , T_B , $\log g_B$ and $(L_B/L_A)_{Bol}$), presenting a worse fit with systematic deviations, reflected by σ (mag) in Table 7.

There are many possible reasons for this, ranging from the difference in the site (PDO is only at 1860 m above sea level and in a much more humid region than SAT at ESO) to the different filters and photomultipliers used. As discussed in Vaz et al. (1997), we believe that this problem is mostly due to the transmission curve of the PDO u filter, which does not match that for the SAT instrumental system. On the other hand, the u light curve solutions are almost always problematic, often not

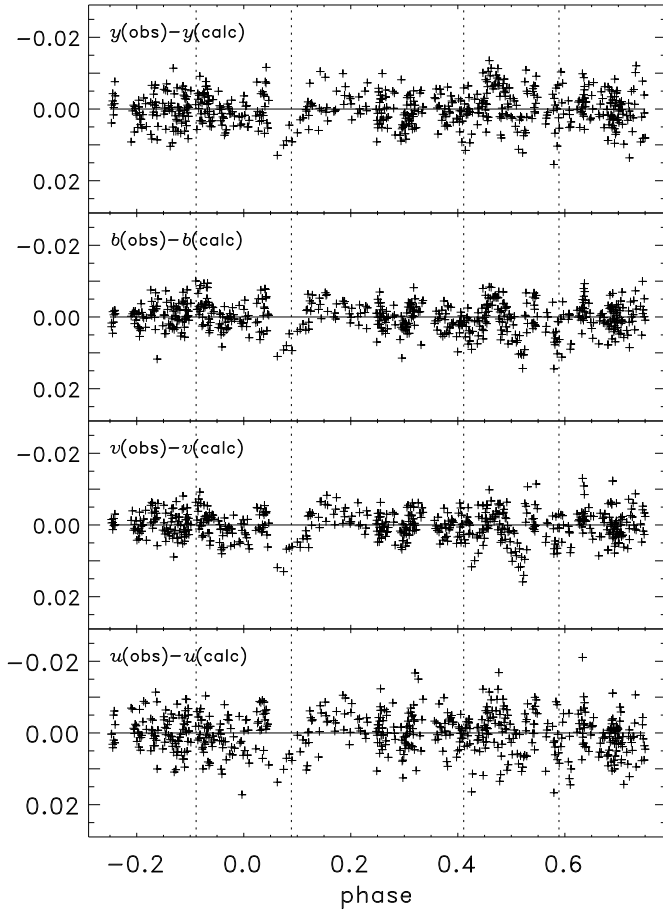


Fig. 4. Residuals of the SAT *uvby* observations from the theoretical light curves (last column of Table 7 and Table 8). The dotted lines delimit the start and end of both eclipses.

Table 8. Mean elements for V 3903 Sgr.

i	$65^{\circ}20 \pm 0^{\circ}07$	M_B/M_A	0.699 ± 0.010
Ω_A	3.49 ± 0.01	r_A mean	0.370 ± 0.003
Ω_B	3.70 ± 0.01	r_B mean	0.280 ± 0.002
$T_{\text{eff},B}/T_{\text{eff},A}$	0.899 ± 0.006	$(T_A=38\,000\text{ K}$	assumed)
L_B/L_A	$0.491 (y)$	$0.488 (b)$	$0.488 (v)$ $0.471 (u)$

agreeing with the solutions for longer wavelengths. Supported by the fact that there is a good agreement between solutions for SAT data and for the *vby* light curves from PDO, and that there is a large number of high-quality solutions based on SAT observations (the Copenhagen Group project), we use only SAT data in our final solution and in the discussion below.

Both components seem to be rotating synchronously with the orbit (Table 7) and are inside their Roche lobes, with the fill-out factors (Mochnacki 1984) being $F_{\text{out},A} = 0.923 \pm 0.009$ and $F_{\text{out},B} = 0.907 \pm 0.011$ and the system being detached. Since there is no evidence of mass exchange (no period changes), the components should be representative for evolutionary studies of single stars.

Table 9. Individual standard indices, not corrected for reddening

star	V	$(b - y)$	m_1	c_1
A	7.705	0.184	0.006	-0.114
B	8.477	0.191	0.001	-0.076

Solution (7) of Table 7 was done with the “spectroscopic” parameters a (semi-major axis), V_γ (center of mass velocity) and q (mass ratio) free to be adjusted by the least-squares method together with the “photometric” parameters i (orbital inclination), Ω_A , Ω_B (gravitational potentials), T_B (temperature of the secondary), and $\mathcal{L}_{A,uvby}$ (model luminosity of the primary). It agrees very well with solutions (1), (2), (4) and (6), considering that the formal errors quoted are a lower limit for the uncertainty in the parameters. Solution (7) is also in excellent agreement with the spectroscopic solutions of Table 4 (Sect. 2).

All sets of solutions of Table 7 do reproduce the observed light curves quite well, excepting PDO *u* light curve, and the rms scatter of the observations from the solutions are comparable to the typical rms errors of the observations (Sect. 3.2). The largest uncertainty is for the values for the luminosity ratios, but the values in Table 7 agree with the spectroscopic determination of Sect 2.2 from the equivalent widths of He I lines. We adopt solution (7), performed for all the 4 colours simultaneously with the radial-velocity curves for both components (Table 3), as our final solution and Table 8 gives the final mean elements for V 3903 Sgr. The O-C residuals for the four colours (SAT observations) and the final solution are shown in Fig. 4, where no systematic trends can be noticed. The O-C between the final solution (adjusted only in the model normalization parameters, magnitude at quadrature and central phase of the primary minimum) for PDO observations show larger and systematic deviations for the *u* colour, evident in Fig. 1 of Vaz et al. (1997).

4. Absolute dimensions and evolutionary status

By using the standard indices (Table 1) and the luminosity ratios for the components (Table 8) we calculate the individual standard indices given in Table 9 (uncorrected for the interstellar reddening). Combining these with unreddened indices for O7V and O9V stars from Crawford (1975), we find a colour excess of $E(b - y) = 0^m.32$, the same value obtained with the mean dereddened colours by Philip & Egret (1983). This is slightly lower than $0^m.33$, found for V 3903 Sgr by Herbst et al. (1982), but definitely inside the errors and in better agreement with colour excesses determined for other member stars of the R association Simeis 188. The absorption $A_V (= 4.28 E(b - y))$, Crawford & Mandwewala 1976) is then $1^m.37$, in full agreement with our previous estimation (Sect. 3.3.1).

We do not find any need for an anomalous law for the interstellar absorption, as Schultz & Wiemer (1975) found for HD 164 865, probably because V 3903 Sgr is not very close to the center of the Lagoon Nebula complex. Torres (1987) also assumes a normal interstellar extinction law towards NGC 6530. As there are less steps and approximations in the derivation

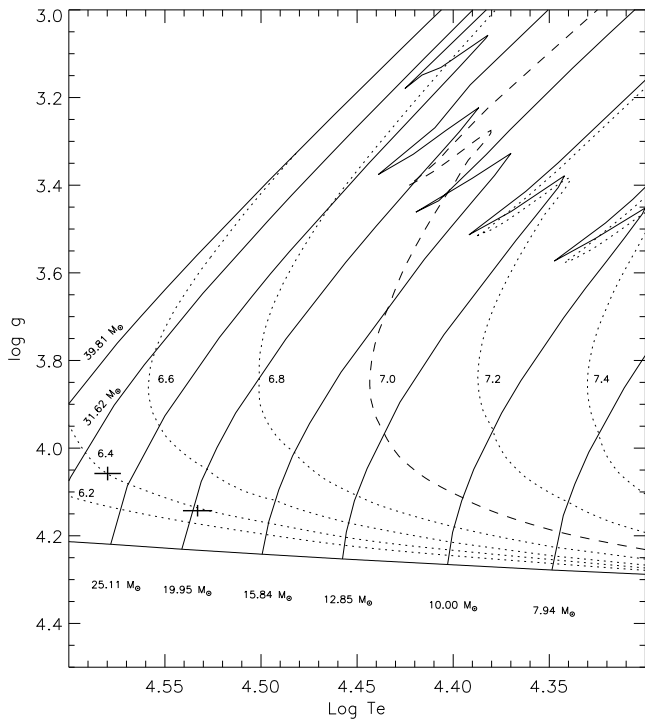


Fig. 5. Evolutionary diagram $\log g$ versus $\log T_{\text{eff}}$ from Claret & Giménez (1992) and the components of V 3903 Sgr. The solid lines represent the evolutionary tracks for each mass while the other lines are the isochrones, labeled in $\log \text{age}(\text{yr})$.

above, we consider it to be more reliable than the former one. Taking this into account, together with bolometric corrections estimated from Popper (1980), we can use our results (Table 8) to calculate the absolute dimensions of the system and estimate its distance. The relevant results are shown in Table 10.

Fig. 5 shows both components of V 3903 Sgr (with 1σ error bars) in the $\log g$ vs. $\log T_{\text{eff}}$ diagram, together with the tracks and isochrones from Claret & Giménez (1992) models for solar composition, considering mass loss and convective overshooting. The components are well represented by the models both in the tracks for the individual masses and by a unique isochrone, giving the theoretical age for the system at $\approx 2.5 \times 10^6$ yrs ($\log \text{age}(\text{yr}) \approx 6.4$), practically the same age of the young cluster NGC 6530. The theoretical effective temperatures at the predicted evolutionary stages agree with the values of Table 10.

The ratio $T_{\text{eff,B}}/T_{\text{eff,A}}$ is determined with an error $<0.7\%$ (Table 8), but the existing temperature calibrations for O stars are claimed to be accurate only to $\pm 5\%$ (Hilditch et al. 1996), these being the errors quoted in Table 10. However, our results are consistent to a much higher precision: there is a common isochrone for the system, and the individual evolutionary tracks match the determined masses, even assuming temperature errors as small as $\approx 1.4\%$ in Table 10, as shown in Fig. 5, where the error bars plotted are for the ± 600 K limit.

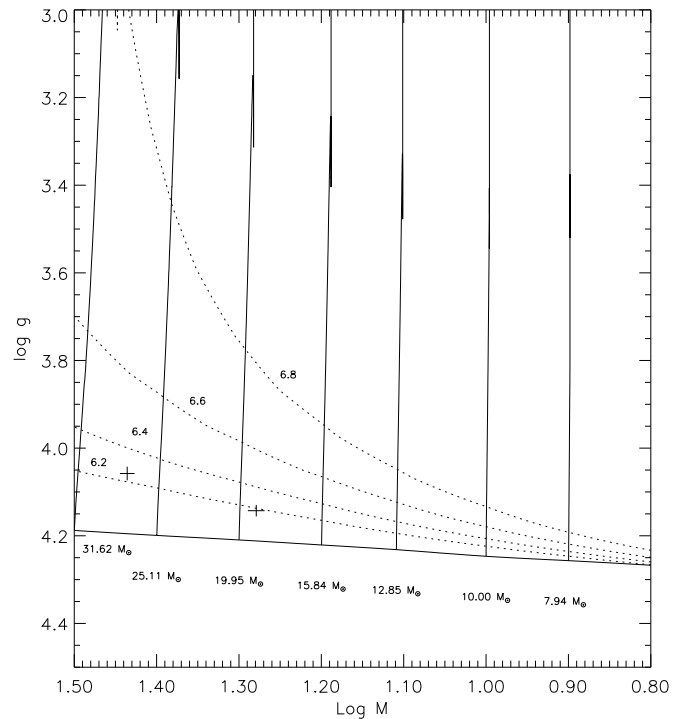


Fig. 6. Evolutionary diagram $\log g$ versus $\log M$ from Claret (1995) and the components of V 3903 Sgr. The solid lines represent the evolutionary tracks for each mass while the dotted lines are the isochrones, labeled in $\log \text{age}(\text{yr})$.

Recently (Claret 1995), a different approximation for mass loss (Nieuwenhuijzen & de Jager 1990) was introduced for models with initial masses above $10M_{\odot}$ during the main sequence stage, and this has consequences for both components of V 3903 Sgr, mainly in their theoretical ages. As can be seen from Fig. 6, the larger mass loss of these new models place both components at the significantly younger age of 1.6×10^6 yrs ($\log \text{age}(\text{yr}) \approx 6.21$), as compared with the age given by the 1992 models. The tracks for the calculated masses match both components at the correct theoretical temperatures and with a unique isochrone, showing again very consistent results.

4.1. Possible membership of a complex structure

The ages quoted for NGC 6530 range from $\log \text{age}(\text{yr})=6.3$ (Battinelli & Capuzzo-Dolcetta 1991, Sagar et al. 1986) to 6.5 (Strobel et al. 1992). The latter work estimates the apparent distance modulus of NGC 6530 as $m-M \sim 12^m 7$. Using our estimation of A_V (which yields $m-M \sim 12^m 3$), both these ages and distances are in a good agreement with our results.

V 3903 Sgr is $\sim 1^{\circ} 17'$ off the center of NGC 6530, and this represents a projected distance of ~ 30 pc. The diameter of NGC 6530 is $\sim 14'$ (~ 6.2 pc, Battinelli & Capuzzo-Dolcetta 1991). Although reasonably far from the center of the cluster, the near equality of the distances and ages indicates that probably V 3903 Sgr is a member of the complex containing NGC 6530 and the Lagoon Nebula (M8).

Table 10. Astrophysical data for V 3903 Sgr.

	A (Primary)	B (secondary)
Absolute dimensions:		
mass (M_{\odot})	27.27 ± 0.55	19.01 ± 0.44
radius (R_{\odot})	8.088 ± 0.086	6.125 ± 0.060
$\log g$ (cgs)	4.058 ± 0.016	4.143 ± 0.013
Rotation Velocities:		
observed (km/s)	230 ± 23	170 ± 17
synchronized (km/s)	228.8 ± 2.4	169.6 ± 1.7
Photometric data:		
T_e (K)	$38\,000 \pm 1\,900$	$34\,100 \pm 1\,700$
M_{bol}	$-8^{\text{m}}03 \pm 0^{\text{m}}07$	$-6^{\text{m}}96 \pm 0^{\text{m}}08$
$\log L/L_{\odot}$	5.087 ± 0.029	4.658 ± 0.032
B.C.	$-3^{\text{m}}44$	$-3^{\text{m}}27$
M_V	$-4^{\text{m}}59 \pm 0^{\text{m}}07$	$-3^{\text{m}}69 \pm 0^{\text{m}}08$
$E(b-y)$		$0^{\text{m}}32$
Distance (pc)	1497 ± 38	

4.2. Circularization and synchronization times

Eclipsing binary systems as close as V 3903 Sgr are good candidates for the study of internal stellar structure. One consequence of the rotational distortions is the exchange between the orbital angular momentum and the spin angular momentum due to the viscosity of the stellar material, yielding the circularization of the orbit and the synchronization of the rotation of each component. Systems with short periods systematically present both small eccentricities (Batten et al. 1989, Duquenooy and Mayor 1991, Latham et al. 1988, 1992) and synchronous rotation of its components with the orbital motion (Kreiken 1935, Swings 1936, Levato 1976, Abt and Levy 1959, Giuricin et al. 1984a,b, Schneider 1986, Tan 1986). This is a sign of tidal forces acting on the systems.

There are currently two approaches with respect to the tidal interactions on radiative stars like the components of V 3903 Sgr. According to one of them (Zahn 1975, 1977, 1984), a periodic external potential induces forced oscillations on the external radiative envelope of the star, which in turn dissipates energy near the stellar surface by radiative damping. The other interpretation treats the effect as a purely hydrodynamical mechanism (Tassoul 1987, 1988, 1990) based on large scale meridional flows.

Since tidal forces depend very sensitively on the stellar dimensions, only binary systems with absolute dimensions accurately determined are suitable to test the models. V 3903 Sgr is such a system, especially interesting not only for the massive components and their consequent rapid evolution, but for the significant difference in the components' masses, also, permitting a precise age determination by fitting an isochrone to the stars. The characteristic time scales were integrated following Claret et al. (1995, Claret and Cunha 1997): τ_{circ} , the time when the eccentricity should vanish (circularization), and τ_{sync} , when each component became synchronized with the orbital period. The results are given in Table 11.

Table 11. Logarithm of critical ages (yrs) for circularization and synchronization for V 3903 Sgr.

	Tassoul	Zahn
$\log \tau_{\text{circ}}$	5.71	6.23
$\log \tau_{\text{sync},A}$	4.94	5.28
$\log \tau_{\text{sync},B}$	4.97	5.28

Despite the system's short age, $\log(\text{age}) \approx 6.2$, the actual orbital eccentricity and rotation for both components do agree very well with both formulations mentioned above. The hydrodynamical mechanism, as proposed by Tassoul, is clearly more efficient than the conventional tidal theory during the main-sequence phase, but this result must be taken with care since the very existence of this mechanism is controversial (Rieutord 1992, Rieutord & Zahn 1997).

5. Conclusions

Our analysis indicates that this is one of the rare detached systems in this spectral range, with the components still close to the ZAMS: the evolutionary models by Claret and Giménez (1992) yield an age of 2.5×10^6 yrs, while new models by Claret (1995) indicate an even younger system at an age of 1.6×10^6 yrs. Both sets of models were calculated with the chemical composition ($X=0.70$, $Z=0.02$), and with core overshooting.

Amongst the well known (errors in the absolute dimensions $\lesssim 2\%$) systems with both components having $M > 17M_{\odot}$, V 3903 Sgr is about the youngest, the one with the most massive primary and where the masses of the components are most different (important in studies of evolutionary tracks). The other systems are EM Car, $M_A = 22.9M_{\odot}$, $M_B = 21.4M_{\odot}$, $\log(\text{age}) \sim 4.5-5 \times 10^6$ yrs (Andersen & Clausen 1989) and Y Cyg, $M_A = 17.5M_{\odot}$, $M_B = 17.3M_{\odot}$, $\log(\text{age}) \sim 2-3 \times 10^6$ yrs (Simon et al. 1994, Hill & Holmgren 1995). DH Cep (Hilditch et al. 1996) is a non-eclipsing ellipsoidal variable at approximately the same age as V 3903 Sgr and with larger masses ($M_A = 32.7M_{\odot}$, $M_B = 29.8M_{\odot}$) but with uncertainties $\sim 5\%$ due almost entirely to the determination of the orbital inclination (at $i=47^\circ$, a 1° error results in a 5% change in the masses).

The calibration for effective temperatures and absolute magnitudes for $T_{\text{eff}} > 30\,000$ K is problematic, due to the lack of reliable empirical determinations in this interval. Schönberner & Harmanec (1995) present a calibration for $10\,000 \text{ K} < T_{\text{eff}} < 30\,000 \text{ K}$. In their study they included preliminary absolute dimensions of V 3903 Sgr (Vaz et al. 1993), but the results were not included in their calibration because they were not very consistent. The intrinsic values of $(b-y)_0$, $\theta(=5.040/T_{\text{eff}})$ and M_V , obtained using Tables 9 and 10 and $E(b-y)=0.32$ (Sect. 4), are presented in Table 12. The definitive absolute dimensions determined in the present work place both components so nicely in the diagrams presented by Schönberner & Harmanec (1995) that we dare suggesting Table 12 as an addition for their Table 2 (which should replace the corresponding entries in the Table 3 of Philip & Egret 1980), ex-

Table 12. Calibrated $(b - y)_0$, $\theta (= 5040/T_{\text{eff}})$ and absolute visual magnitude for the components of V 3903 Sgr.

star	$(b - y)_0$	θ	M_V
A	-0.136	0.133	-4.59
B	-0.129	0.148	-3.69

tending the range of effective temperatures of their calibration up to 38000 K. V 3903 Sgr is one of the least evolved systems at this mass range and we believe that the present solution is rather robust.

The preliminary absolute dimensions of V 3903 Sgr (Vaz et al. 1993) were also used by Hilditch et al. (1996), and the inconsistency detected by Schönberner & Harmanec was again noted. However, the definitive solutions presented here are fully consistent, also when analysed with the evolutionary models of Schaller et al. (1992), used by Hilditch et al. (1996) to interpret DH Cep, which somewhat confirms an age of $\sim 1.6 \times 10^6$ yrs for V 3903 Sgr.

The circular orbit and the synchronized intrinsic rotation velocities can be explained theoretically, despite the short age of the system. For both models by Claret & Giménez (1992) and Claret (1995) it was possible to find an isochrone for the system and individual evolutionary tracks that matched very well the results for both components. No sign of mass transfer could be detected through period changes and the absolute parameters for the non-interacting components of V 3903 Sgr should then be representative for single stars of the same mass.

V 3903 Sgr is important for the study of stellar evolutionary models, due to its very massive (but having different masses) and young components. Besides, being a member of the R association Simeis 188 (Herbst et al. 1982), the illuminating star of the bright nebula IC 4685 (Hirshfeld & Sinnott 1982, 1985), and very possibly a physical member of the Lagoon Nebula Complex (Messier 8 and NGC 6530), V 3903 Sgr is an important object for the study of this complex structure, also, where star formation still is going on (Stahler 1985).

Acknowledgements. This work has been supported by the Brazilian institutions: FAPEMIG, CNPq, FINEP, CAPES. LPRV acknowledges (CNPq) support received while being a visiting scientist at the Department of Astronomy, University of Wisconsin, Madison, and is grateful for the hospitality received there from Aug 1993 to Oct 1994, while part of this paper was completed. Fruitful discussions with Dr. Jens Viggo Clausen and a careful reading by Dr. Dave Stickland are gratefully acknowledged. This research has made use of the Simbad data base, operated by the CDS, Strasbourg, France. A substantial part of the computations was done under LINUX (a GNU Public Licence UNIX operating system clone).

References

- Abt H.A., Levy S.G., 1959, ApJS 59, 229
Aitken R., 1964, in The Binary Stars, Dover reprint, New York, Chap. VI
Alencar S.H.P., Vaz L.P.R., Helt B.E., 1997, A&A, in press
Andersen J., 1975, A&A 44, 445
Andersen J., 1993, A&ARS 3, 91
Andersen J., Clausen J.V., 1989, A&A 213, 183
Andersen J., Clausen J.V., Nordström B., 1980, in Close Binary Stars Observations and Interpretation (IAU Symp. 88), eds. M.J. Plavec, D.M. Popper, R.K. Ulrich. Reidel, Dordrecht, p. 81
Balona L.A., 1990, ASP Conference Series 11, 245
Batten A.H., Fletcher J.M., McCarthy D.G., 1989, Publ. Dominion Astrophys. Obs. 17, 1
Battinelli P., Capuzzo-Dolcetta R., 1991, MNRAS 249, 76
Binnendijk L., 1960, in Properties of Double Stars, Univ. of Pennsylvania, p. 163
Casey B.W., Mathieu R.D., Suntzeff N.B., Lee C.-W., Cardelli J.A., 1992, AJ 105, 2276
Claret A., 1995, A&AS 109, 441
Claret A., Cunha N.C.S., 1997, A&A 318, 187
Claret A., Giménez A., 1992, A&AS 96, 255
Claret A., Giménez A., Cunha N.C.S., 1995, A&A 299, 724
Clariá J.J., 1976, IBVS 1106
Conti P.S., 1973, ApJ 179, 181
Conti P.S., Alschuler W.R., 1971, ApJ 170, 325
Cousins A.W.J., 1973, Mon. Notes Astron. Soc. S. Afr. 32, 11
Crawford D.L., 1975, PASP 87, 481
Crawford D.L., Mandwewala N., 1976, PASP 88, 917
Cunha N.C.S., 1990, M. Sci. Dissertation, Physics Dept., Exact Sci. Inst., Federal Univ. of Minas Gerais, Brazil
Cunha N.C.S., Vaz L.P.R., Pössa C.M.M., Helt B.E., Clausen J.V., 1990, IBVS 3436
Díaz-Cordobés J., Giménez A., 1992, A&A 259, 227
Duquennoy A., Mayor M., 1991, A&A 248, 485
Etzell P.B., 1985, "SBOP - Spectroscopic Binary Orbit Program", Program's Manual
Giménez A., Clausen J.V., Andersen A., 1986, A&A 160, 310
Giuricin G., Mardirossian F., Mezzetti M., 1984a, A&A 131, 152
Giuricin G., Mardirossian F., Mezzetti M., 1984b, A&A 135, 393
Herbst W., Miller D.P., Warner J.W., Herzog A., 1982, AJ 87, 98
Hilditch R.W., Harries T.J., Bell S.A., 1996, A&A 314 165
Hill G., Holmgren D.E., 1995, A&A 297, 127
Hill G., Khallesseh B., 1991, A&A 245, 517
Hiltner W.A., Johnson H.L., 1956, ApJ 124, 367
Hirshfeld A., Sinnott R.W., 1982, Sky Catalogue 2000.0, Vol. 1, Cambridge Univ. Press and Sky Publishing Co.
Hirshfeld A., Sinnott R.W., 1985, Sky Catalogue 2000.0, Vol. 2, Cambridge Univ. Press and Sky Publishing Co.
Janot-Pacheco E., Leister N.V., Quast G.R., Torres C.A.P. C.O. 1991, in ESO Workshop, "Rapid Variability of OB Stars: Nature and Diagnostics Value", Baade D. (ed.), Garching, p. 45
Horne K., 1986, PASP 98, 609
Kreiken E.A., 1935, Zs. für Ap. 10, 199
Kurucz R.L., 1979, ApJS 40, 1
Kwee K.K., Van Woerden H., 1956, Bull. Astron. Inst. Neth. 12, 327
Lafleur J., Kinman T.D., 1965, ApJS 11, 216
Lamers H.J.G.L.L., 1981, ApJ 245, 593
Latham D.W., Mazeh T., Carney T., McCrosky B.W., Stefanik R.E., Davis R.P., 1988, AJ 96, 567
Latham D.W., Mazeh T., Stefanik R.E., Davis R.P., Carney T., Kromolowsky Y., Laird J.B., Torres G., Morse J.A., 1992, AJ 104, 774
Laurenti M.A., Cerruti M.A., 1990, IBVS 3463
Lehmann-Filhes R., 1894, AN 163, 17
Lester J.B., Gray, R.O., Kurucz, R.L., 1986, ApJS 509
Levato H., 1976, ApJ 203, 680
Mochnacki S.W., 1984, ApJS 55, 551

- Morton D.C., 1969, *ApJ* 158, 629
- Myrrha M.L.M., 1991, M. Sci. Dissertation, Physics Dept., Exact Sci. Inst., Federal Univ. of Minas Gerais, Brazil
- Napiwotzki R., Schönberner D., Wenske V., 1993, *A&A* 268, 653
- Nielsen R.F., Nørregaard P., Olsen E.H., 1987, *ESO Messenger* 50, 45
- Niemela V., Morrison N.D., 1988, *PASP* 100, 1436
- Nieuwenhuijzen H., de Jager C., 1990, *A&A* 231, 134
- Philip A.G.D., Egret D., 1980, *A&AS* 40, 199
- Philip A.G.D., Egret D., 1983, *A&A* 123, 39
- Popper D.M., 1980, *ARA&A* 18, 115
- Popper D.M., Etzel P.B., 1981, *AJ* 86, 102
- Reid A.H.N., Bolton C.T., Crowe R.A., Fieldus M.S., Fullerton A.W., Gies D.R., Howarth I.D., McDavid D., Prinja R.K., Smith K.C. 1993, *ApJ* 417, 320
- Rieutord M., 1992, *A&A* 259, 581
- Rieutord M., Zahn J.-P., 1997, *ApJ* 474, 760
- Russell H.N., 1902, *ApJ* 15, 252
- Sagar R., Piskunov A.E., Myakutin V.I., Joshi U.C., 1986, *MNRAS* 220, 383
- Schaller G., Schaerer D., Meynet G., Maeder A., 1992, *A&AS* 96, 269
- Schneider H., 1986, in: *Upper Main Sequence Stars with Anomalous Abundances*, Cowley, C.R., Dworetzky, M.M., Mégessier, C. (eds.), Dordrecht:Reidel, p. 205
- Schönberner D., Harmanec P., 1995, *A&A* 294, 509
- Schultz G.V., Wiemer W., 1975, *A&A* 43, 133
- Seaton M.J., 1979, *MNRAS* 187, 73P
- Simon K.P., Sturm E., Fiedler A., 1994, *A&A* 292, 507
- Slettebak A., Collins G.W.II, Boyce P.B., White N.M. Parkinson I.D., 1975, *ApJS* 281, 137
- Stahler S.W., 1985, *ApJ* 293, 207
- Sterne T.E., 1941, *Harvard Univ. Astron. Obs. Reprint* 222
- Stickland D., 1996, personal communication
- Strobel A., Skaba W., Proga D., 1992, *A&A* 245, 75
- Swings P., 1936, *Zs. für Ap.* 12, 40
- Tan H.S., 1986, *Chin. Astron. Astrophys.* 10, 54
- Tassoul J.-L., 1987, *ApJ* 322, 856
- Tassoul J.-L., 1988, *ApJ* 324, L71
- Tassoul J.-L., 1990, *ApJ* 358, 196
- Torres A.V., *ApJ* 322, 949
- Van Hamme W., 1993, *AJ* 106, 2096
- Van Hamme W., 1995, personal communication
- Vaz L.P.R., 1986, *Rev. Mex. Astron. Astrofis.* 12, 199
- Vaz L.P.R., Andersen A., Rabello Soares M.C.A., 1995, *A&A* 301, 631
- Vaz L.P.R., Cunha N.C.S., Vieira E.F., Myrrha M.L.M., 1993, *ASP Conference Series* 40, 371
- Vaz L.P.R., Cunha N.C.S., Andersen J., Clausen J.V., Garcia J.M., Giménez A., Casey B.W., de Koff S., 1997, submitted to *A&AS*
- Vieira E.F., 1991, M. Sci. Dissertation, Physics Dept., Exact Sci. Inst., Federal Univ. of Minas Gerais, Brazil
- Vieira E.F., 1993, *Trabajo de Investigación del Tercer Ciclo*, Astrophysics Dept., Universidad Complutense de Madrid, Spain
- von Zeipel H., 1924, *MNRAS* 24, 665
- Wade R.A., Ruciński S.M., 1985, *A&AS* 60, 471
- Walker G.A.H., Moyles K., Yang S., Fahlman, G.G., 1979, *ApJ* 233, 199
- Wilsing J. 1893, *Astron. Nachr.* 134, 90
- Wilson R.E., 1979, *ApJ* 234, 1054
- Wilson R.E., 1993, in *New Frontiers in Interacting Binary Star Research*, eds. K.C. Leung and I.-S. Nha, *ASP Conf. Series* 38, 91
- Wilson R.E., Devinney E.J., 1971, *ApJ* 182, 539
- Wilson R.E., Sofia S., 1976, *ApJ* 203, 182
- Wolfe Jr. R.H., Horak H.G., Storer N.W., 1967, in *Modern Astrophysics*, ed. M. Hack, Gauthiers-Villars, Paris, and Gordon and Breach, New York, p. 251
- Wood D.B., 1971, *AJ* 76, 701
- Zahn J.-P., 1975, *A&A* 41, 329
- Zahn J.-P., 1977, *A&A* 57, 383
- Zahn J.-P., 1984, in: *Observational Tests of the Stellar Evolution Theory*, Maeder, A., Renzini, A. (eds.), pp 379-389